ORGANOMETALLICS

Article

pubs.acs.org/Organometallics

Diamido-Ether Actinide Complexes as Initiators for Lactide Ring-Opening Polymerization

Cassandra E. Hayes,[†] Yann Sarazin,[‡] Michael J. Katz,[§] Jean-François Carpentier,[‡,*] and Daniel B. Leznoff[†,*]

[†]Department of Chemistry, Simon Fraser University, 8888 University Drive, Burnaby, British Columbia, Canada V5A 1S6

[‡]Institut des Sciences Chimiques de Rennes, UMR 6226 CNRS, Université de Rennes 1, Campus de Beaulieu, 35042 Rennes Cedex, France

[§]Department of Chemistry, Northwestern University, 2145 Sheridan Road, Evanston, Illinois, United States 60208-3113

Supporting Information

ABSTRACT: The synthesis and characterization of a series of new diamido-ether actinide(IV) alkoxide complexes are reported. Addition of 2 equiv of LiO^{i}Pr to [^{tBu}NON]-ThCl$_5$Li$_3$·DME ([^{tBu}NON]$^{2-}$ = [(^{t}BuNSiMe$_2$)$_2$O]$^{2-}$) in toluene gives [^{tBu}NON]Th(O^{i}Pr)$_3$Li·DME (**1-DME**). Recrystallization of **1-DME** from diethyl ether gives [^{tBu}NON]Th-(O^{i}Pr)$_3$Li·Et$_2$O (**1-Et$_2$O**). The addition of 2 equiv of LiO^{i}Pr to {[^{tBu}NON]UCl$_2$}$_2$ gives {[^{tBu}NON]U(O^{i}Pr)$_2$}$_2$ (**2**). If KO^{t}Bu is used instead, the product is {[^{tBu}NON]U(O^{t}Bu)}$_2$ (**3**). The reaction of 2 equiv of KO^{t}Bu with [^{iPr_2Ph}NCOCN]ThCl$_2$·DME ([^{iPr_2Ph}NCOCN]$^{2-}$ = [(2,6-^{i}Pr$_2$PhNCH$_2$CH$_2$)$_2$O]$^{2-}$) gives [^{iPr_2Ph}NCOCN]Th(O^{t}Bu)$_2$ (**4**), while addition of 1 equiv of KO^{t}Bu to [^{iPr_2Ph}NCOCN]UCl$_3$Li·THF results in [^{iPr_2Ph}NCOCN]U(O^{t}Bu)Cl (**5**). Complexes **1**−**5** as well as the previously reported diamido actinide dialkyl complexes [^{tBu}NON]An(CH$_2$SiMe$_3$)$_2$ (An = Th (**6**), U (**7**)) and [^{iPr2Ph}NCOCN]An(CH$_2$SiMe$_3$)$_2$ (An = Th (**8**), U (**9**)) were evaluated as initiators for the ring-opening polymerization (ROP) of L-lactide (L-LA) and racemic lactide (*rac*-LA). It was established that complexes **1**−**8** were capable of producing poly(L-LA) (PLLA) under mild conditions within relatively short periods of time. Diisopropoxide complex **2** polymerized up to 500 equiv of L-LA in 90 min at 30 °C, with moderate to good control over the molecular weight features (values of M_w/M_n with this complex are typically 1.5 or below). The hydrocarbyl complexes **6**−**8** also proved active under the same conditions, with **7** showing a similar ability to control the ROP with monomer loadings up to 500 equiv. PLLAs prepared with initiators **1**−**5** and **6**−**8** have been characterized by end-group analysis via NMR and MALDI-TOF MS, which indicate clearly that the diamido ligand does not participate as an initiating group in the ROP process and that the alkoxide and alkyl moieties, respectively, are the only initiating groups. When it was applied to mediate the ROP of *rac*-LA, **2** yielded heterotactically enriched PLA (P_r values up to 0.73 in THF).

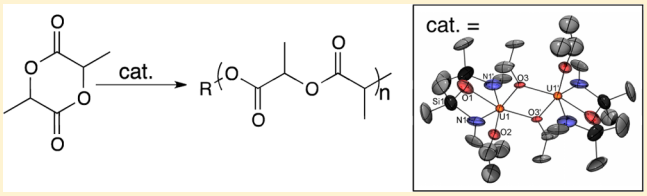

INTRODUCTION

A large number of efficient oxophilic metal-based complexes have been reported over the past two decades for the ring-opening polymerization (ROP) of cyclic esters such as ϵ-caprolactone, L and racemic lactide (L-LA, *rac*-LA) and racemic β-butyrolactone.[1] Many of these catalysts display high control over the polymerization parameters, and a number of them have been reported to facilitate the production of highly stereoregular polylactide (PLA) by stereocontrolled ROP of *rac*-LA. A range of different ligand frameworks that support these metal catalysts have been described. Ancillary ligands based on anionic phenoxide donors further supported by neutral, potentially hemilabile donors such as amines and ethers have been very popular in these studies.[2] Nitrogen-based ligands in the form of β-diketiminates or weakly donating sulfonamides and phosphinamides also proved to be highly effective frameworks for metal complexes that facilitated the controlled ROP of lactides.[3] Some reports of strictly amide-based complexes that show good performance for such ROPs are also available.[4]

In comparison with the large amount of work that has been done targeting lanthanide-based ROP catalysts,[1] reports of the use of actinide complexes for the ROP of cyclic esters are very scarce.[5] Generally speaking, actinide metals exhibit a number of properties that make them good candidates for use in catalysis: namely, access to an enlarged coordination sphere, the possibility of f-orbital participation, and access to a number of oxidation states.[6] There has indeed been considerable work in the advancement of actinide-based catalysts in general, as highlighted in several recent reviews.[6b,d,7] Until recently, actinide alkoxide complexes were not expected to be viable for the catalysis of organic transformations due to the high oxophilicity of the actinide centers; however, several reports

Special Issue: Recent Advances in Organo-f-Element Chemistry

Received: October 22, 2012
Published: February 11, 2013

dx.doi.org/10.1021/om300993r | *Organometallics* 2013, 32, 1183−1192

have now shown that actinide-based alkoxide complexes are in fact active in a variety of catalytic cycles.[5,8] In particular, $Cp^*_2AnMe_2$ (An = Th, U) and $[U(NEt_2)_3][BPh_4]$ have shown activity as catalysts for the ROP of ε-caprolactone and L-LA.[5a] In another related example, $Cp^*_2ThMe_2$ ($Cp^* = C_5Me_5$), $Me_2SiCp'_2Th(C_4H_9)_2$, and $Th(NEtMe)_4$ precatalysts have been used to promote the dimerization of a large number of aldehydes to give the corresponding esters.[8a,c] These precatalysts incorporate alkyl or amide moieties, but mechanistic studies have indicated that, prior to entering the catalytic cycle for aldehyde dimerization, these groups are replaced by alkoxide substituents from the incoming aldehydes.[8c]

A number of isolated homoleptic actinide alkoxide[9] and heteroleptic actinide alkoxide complexes have been reported.[8c,9b,d,f,10] In addition, the use of cyclopentadienyl-free actinide complexes for catalytic applications lags behind that of the Cp*-based analogues, leaving considerable room for additional studies and possible improvement in the design of actinide catalyst systems. Of particular interest to us, amido-based actinide(IV) complexes have shown increasing promise for catalytic applications, including reports of olefin polymerization and hydroamination.[10o,11] As such, we sought to apply diamido-ether actinide complexes developed in our laboratory for use as initiators in the ROP of lactide, a monomer of growing academic and industrial significance.

Thus, herein we report the synthesis of a new series of diamido-ether actinide alkoxide heteroleptic complexes containing the $[(^tBuNSiMe_2)_2O]^{2-}$ ($[^{tBu}NON]^{2-}$) and $[(^iPr_2PhNCH_2CH_2)_2O]^{2-}$ ($[^{iPr_2Ph}NCOCN]^{2-}$) ligand frameworks. The activities of these complexes and several previously reported diamido-ether actinide dialkyls,[11c,12a,13] specifically $[^{tBu}NON]An(CH_2SiMe_3)_2$ (An = Th (**6**), U (**7**)) and $[^{iPr_2Ph}NCOCN]An(CH_2SiMe_3)_2$ (An = Th (**8**), U (**9**)), for the ROP of L-LA and *rac*-LA are presented. The impact on the control of polymerization as a function of choice of actinide metal and diamido ligand as well as of changes in solvent and temperature is discussed.

RESULTS AND DISCUSSION

Synthesis of Diamido-Actinide Alkoxide Complexes. The synthesis of new diamido actinide alkoxide complexes was achieved through standard salt metathesis reactions of the requisite parent diamido actinide dihalide complex with the appropriate lithium or potassium alkoxide reagent (Scheme 1). Thus, addition of 2 equiv of LiO^iPr to $[^{tBu}NON]ThCl_3Li_3$·DME ($[^{tBu}NON]^{2-} = [(^tBuNSiMe_2)_2O]^{2-}$; DME = 1,2-dimethoxyethane) in toluene gave a cloudy yellow solution that after 18 h and workup resulted in a yellow solid of $[^{tBu}NON]Th(O^iPr)_3Li$·DME (**1-DME**). Unsurprisingly, addition of 3 equiv of LiO^iPr to $[^{tBu}NON]ThCl_3Li_3$·DME resulted in an increase in the yield of **1-DME** to 79%.

Scheme 1. Synthesis of Complexes 1−3

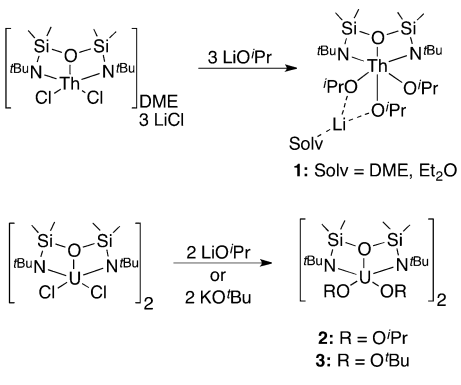

The ^1H NMR spectrum of **1-DME** in toluene-d_8 contains nine resonances at room temperature and is consistent with a C_s-symmetric structure in solution; it indicates retention of the DME molecule even after repeated washing with hexanes and toluene. There are three resonances for the diamido ligand, which has two inequivalent silyl methyl groups. The O^iPr substituents appear as four resonances, consistent with two different environments for these ligands. A doublet at δ 1.26 ppm and a septet at δ 4.59 ppm that integrate respectively to 12H and 2H are consistent with two unhindered $CH(CH_3)_2$ groups. The $^{13}C\{^1H\}$ NMR spectrum of **1-DME** indicates that there are two carbon resonances at δ 28.80 and 28.99 ppm that are coincident in the ^1H NMR spectrum, obscuring the fact that there are actually three different environments for the O^iPr groups. A second multiplet at δ 4.66 ppm that integrates to 1H and a doublet at δ 1.41 ppm that integrates to 6H are observed for the third inequivalent O^iPr group. Finally, two resonances are observed for the coordinated DME molecule.

Variable-temperature ^1H NMR experiments on **1-DME** provide more insight into the overlapping resonances observed in the room-temperature spectrum. Upon cooling from 25 to −80 °C, the ^1H NMR spectrum of **1-DME** broadens as the overlapping resonances begin to separate, and coalescence occurs at −40 °C. Due to the overall broadness of many resonances at the low-temperature limit of −80 °C, full separation of all the resonances was not observed; however, the formerly coincident resonances for the two overlapping $CH(CH_3)_2$ groups which integrated to 12H at δ 1.26 ppm at room temperature have separated into two broad singlets at δ 1.21 and 1.30 ppm. To further confirm this, the multiplet at δ 4.59 ppm at room temperature has also separated into two broad singlets at δ 4.61 and 4.69 ppm at −80 °C. As well, the overlapping resonances for the ^{t}Bu-N and third $CH(CH_3)_2$ groups have also begun to separate but the separation is not as complete as for the other $CH(CH_3)_2$ groups. In this instance, a singlet at δ 1.58 ppm for the ^{t}Bu-N resonance is observed with a broad shoulder that spans the spectrum between δ 1.58 and 1.65 ppm.

Despite multiple attempts to recrystallize **1-DME** from DME or toluene, no single crystals of X-ray quality were obtained; however, recrystallization of **1-DME** via slow evaporation of a diethyl ether solution resulted in the isolation of crystals suitable for X-ray diffraction. The structure of **1** when recrystallized from an Et_2O/toluene solution retains one Et_2O molecule in the product **1-Et$_2$O**. The structure of this adduct **1-Et$_2$O** reveals the thorium atom in a six-coordinate distorted-octahedral environment meridionally coordinated by the tridentate $[^{tBu}NON]^{2-}$ ligand, three isopropoxide ligands, and a solvent-coordinated lithium cation (Figure 1). One of the O^iPr^- substituents is terminally bound to the thorium, while the other two O^iPr^- ligands bridge the thorium and lithium atoms. The lithium exists in a three-coordinate environment that is completed by the coordination of a disordered diethyl ether molecule. The Th(1)−N(10) bond distance of 2.382(12) Å is longer than in $\{[^tBuNON]ThCl_2\}_2$, which has Th−N distances of 2.29(2) and 2.291(19) Å, and longer than the Th−N distances in (2,6-bis(2,6-diisopropylanilidomethyl)pyridine)-$ThCl_2$·DME (2.305(9) and 2.321(8) Å).[12] These Th−N bond lengths are also longer than in monodentate amido thorium

dx.doi.org/10.1021/om300993r | Organometallics 2013, 32, 1183−1192

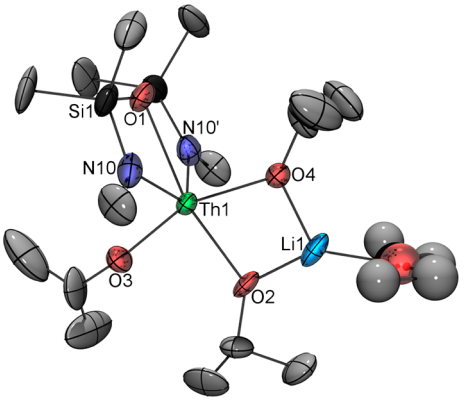

Figure 1. Molecular structure and numbering scheme of **1-Et$_2$O** (thermal ellipsoids shown at 30% probability). Hydrogen atoms are omitted, and ^{t}Bu-N groups are simplified for clarity. Selected bond distances (Å) and angles (deg): Th(1)−N(10), 2.382(12); Th(1)−O(1), 2.652(11); Th(1)−O(2), 2.298(9); Th(1)−O(3), 2.153(10); Th(1)−O(4), 2.285(11); Li(1)−O(2), 1.83(4); Li(1)−O(4), 1.87(3); N(10)−Th(1)−N(10′), 121.3(6); N(10)−Th(1)−O(1), 61.0(3); O(1)−Th(1)−O(2), 165.4(4); O(2)−Th(1)−O(4), 70.4(4); O(3)−Th(1)−O(4), 158.8(4).

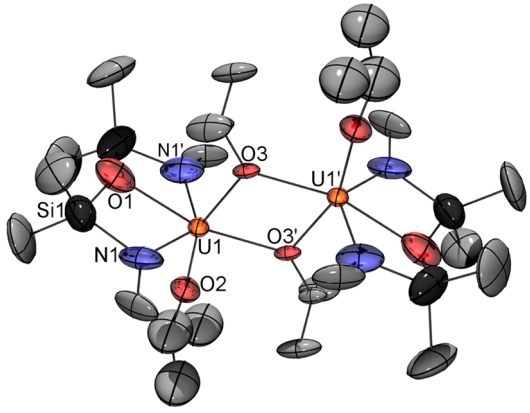

Figure 2. Molecular structure and numbering scheme of **2** (thermal ellipsoids shown at 30% probability). Hydrogen atoms are omitted, and ^{t}Bu-N groups are simplified for clarity. Selected bond distances (Å) and angles (deg): U(1)−N(1), 2.20(2); U(1)−O(1), 2.50(3); U(1)−O(2), 2.12(2); U(1)−O(3), 2.326(17); U(1)···U(1′), 3.895(2); N(1)−U(1)−N(1′), 126.0(13); N(1)−U(1)−O(1), 63.7(6); O(3)−U(1)−O(3′), 67.5(6); O(2)−U(1)−O(3), 158.1(7); O(1)−U(1)−O(3′), 159.6(7).

complexes; for example, Th[N(SiMe$_3$)$_2$]$_2$(NMePh)$_2$ has Th−N distances between 2.299(6) and 2.328(6) Å.[9f] It seems reasonable that the abundance of electron density from the three hard isopropoxide ligands reduces the impetus for increased electron donation from the diamido ligand, resulting in longer Th−N bond lengths in **1·Et$_2$O**. The Th(1)−O(1) bond distance of 2.652(11) Å is also longer than in {[$^{t\text{Bu}}$NON]ThCl$_2$}$_2$, where the Th−O distance is 2.531(17) Å but is more comparable with the Th−O distance of 2.663(13) Å in the "ate" complex {[(Me$_3$PhNSiMe$_2$)$_2$O]-ThCl$_3$Li·THF}$_2$.[12a,13] The Th(1)−O(3) distance (to the terminal O^{i}Pr group) of 2.153(10) Å is similar to the terminal Th−O distances in {Th(O^{i}Pr)$_4$}$_2$, which range from 2.141(11) to 2.160(11) Å, while the bridging Th(1)−O(2) and Th(1)−O(4) distances of 2.298(9) and 2.285(11) Å, respectively, are somewhat shorter than the bridging Th−O distances in {Th(O^{i}Pr)$_4$}$_2$ (2.408(10) Å).[9c]

Addition of 2 equiv of LiO^{i}Pr to {[$^{t\text{Bu}}$NON]UCl$_2$}$_2$ in toluene gave a cloudy green-brown solution that after 18 h and workup resulted in a green-brown powder of {[$^{t\text{Bu}}$NON]U-(O^{i}Pr)$_2$}$_2$ (**2**) in 93% yield (Scheme 1). Crystals of **2** suitable for X-ray diffraction were grown by slow evaporation of a toluene solution. In the solid state, a dimeric structure is observed in which each uranium atom exists in a distorted-octahedral environment supported by the meridionally bound tridentate [$^{t\text{Bu}}$NON]$^{2-}$ ligand, one terminal isopropoxide ligand per uranium and two isopropoxide ligands that bridge the two metal centers (Figure 2); unlike **1**, this system does not retain salt and is not an "ate" complex. The U(1)−N(1) distance of 2.20(2) Å in **2** is slightly longer than in {[$^{t\text{Bu}}$NON]UX$_2$}$_2$ (X = Cl$_{0.54}$/Br$_{0.46}$),[12a] which has U−N distances of 2.145(16) and 2.130(18) Å. However, these U−N distances are more comparable with the U−N distances of 2.224(8) and 2.223(8) Å in {[(^{i}Pr$_2$PhNSiMe$_2$)$_2$O]UCl$_2$}$_2$ and the U−N distances of 2.194(3) and 2.215(4) Å in {(Me$_3$SiN-(CH$_2$CH$_2$NSiMe$_3$)$_2$)UCl$_2$}$_2$.[11c,14] The U(1)−O(1) distance of 2.50(3) Å is also similar to but slightly shorter than the U−O distance in {[(^{i}Pr$_2$PhNSiMe$_2$)$_2$O]UCl$_2$}$_2$ (2.567(7) Å).[11c] The U(1)−O(2) distance of 2.12(2) Å to the terminally bound O^{i}Pr group compares well with the U−O distance for the terminally bound *tert*-butoxide ligands of the homoleptic {Li(THF)}$_2${U-(O^{t}Bu)$_6$} (2.140(8) and 2.137(9) Å).[9g] The bridging U(1)−O(3) distance of 2.326(17) Å also compares well with the bridging U−O−Li distances in {Li(THF)}$_2${U(O^{t}Bu)$_6$}, which range between 2.252(6) and 2.412(8) Å.[9g] This U(1)−O(3) distance is also comparable with the bridging U−O distance of 2.29(1) Å in {U$_2$(O^{i}Pr)$_{10}$}.[9a]

The ^{1}H NMR spectrum of the paramagnetic **2** in benzene-d_6 contains seven broad, highly shifted resonances and is consistent with an overall C_2-symmetric structure in solution. Although not all of the resonances can be assigned on the basis of the integrations, some observations can be made. There are four distinct resonances that each integrate to 6H, indicating that the silyl methyl groups are inequivalent and that there are two environments for the O^{i}Pr substituents; this suggests that the dimeric structure is maintained in solution. The two resonances that integrate to 1H at δ −16.24 and 77.90 ppm can be assigned to the two C*H*(CH$_3$)$_2$ hydrogens, and the resonance at δ −49.55 ppm integrates to 18H and can be assigned to the *tert*-butyl methyl groups of the diamido ligand.

Addition of 2 equiv of KO^{t}Bu to {[$^{t\text{Bu}}$NON]UCl$_2$}$_2$ in toluene gave a light brown solution from which a red-brown solid of {[$^{t\text{Bu}}$NON]U(O^{t}Bu)$_2$}$_2$ (**3**) was isolated in 89% yield (Scheme 1). Crystals of **3** were grown by slow evaporation of a pentane solution, but unfortunately they were not suitable for single-crystal X-ray diffraction. The ^{1}H NMR spectrum of **3** in benzene-d_6 contains four broad, highly shifted resonances typical of paramagnetic complexes. Two of these resonances at δ −44.57 and −42.51 ppm integrate to 6H and can be assigned to the silyl methyl groups. The other two resonances at δ −37.55 and −10.07 ppm both integrate to 18H and are consistent with the *tert*-butyl groups of the diamido ligand and two alkoxide ligands but could not be further assigned.

Addition of two equiv of KO^{t}Bu to [$^{i\text{Pr}_2\text{Ph}}$NCOCN]-ThCl$_2$·DME in DME gave a pale yellow solution from which a light yellow powder of [$^{i\text{Pr}_2\text{Ph}}$NCOCN]Th(O^{t}Bu)$_2$ (**4**) was obtained in 79% yield (Scheme 2). The NMR spectra and microanalysis data are consistent with this formulation, but no X-ray-quality crystals could be obtained. Although no X-ray

dx.doi.org/10.1021/om300993r | *Organometallics* 2013, 32, 1183−1192

Scheme 2. Synthesis of Complexes 4 and 5

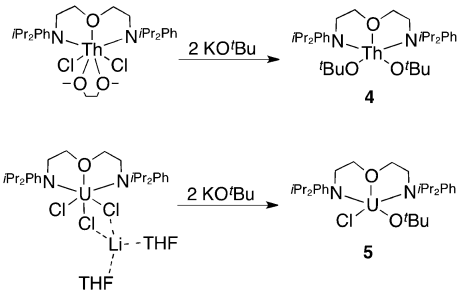

Chart 1. Diamido-Actinide Complexes 1−9 Used in the ROP of Lactide

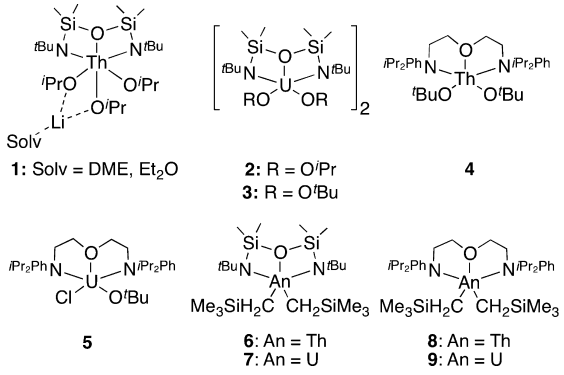

data could be obtained for **4**, previous reports using the [$^{i\mathrm{Pr_2Ph}}$NCOCN]$^{2-}$ ligand indicate that it may coordinate in either a facial[20] or meridional fashion.[11c,13] The ^{1}H NMR spectrum of **4** in toluene-d_8 displays six distinct resonances consistent with a C_{2v}-symmetric structure in solution, suggesting that the ligand is indeed coordinated in a meridional fashion. Notably, the [$^{i\mathrm{Pr_2Ph}}$NCOCN]$^{2-}$ ligand is symmetric and no hindered rotation in the room-temperature ^{1}H NMR spectrum is observed; one doublet integrating to 24H exists for the aryl isopropyl groups, in addition to one septet for the C*H*(CH$_3$)$_2$ hydrogens, two triplets for the backbone CH$_2$ groups, and a multiplet for the aryl hydrogens. One broad resonance that integrates to 18H is also observed for the two *tert*-butoxide groups. The ^{13}C{^{1}H} NMR data also support this formulation (see the Experimental Section).

Addition of 2 equiv of KO^{t}Bu to [$^{i\mathrm{Pr_2Ph}}$NCOCN]-UCl$_3$Li·2THF in toluene gave a red-brown solution that gave after 18 h and workup a red-brown solid of [$^{i\mathrm{Pr_2Ph}}$NCOCN]-U(O^{t}Bu)Cl (**5**) (Scheme 2); however, the product was somewhat impure. In an effort to prepare a purer sample of **5**, the reaction was repeated using 1 equiv of KO^{t}Bu. After workup and isolation (90% yield), a sample of **5** with microanalysis data consistent with the formulation [$^{i\mathrm{Pr_2Ph}}$NCOCN]U(O^{t}Bu)Cl was obtained. The ^{1}H NMR spectrum of **5** in toluene-d_8 contains 10 broad, highly shifted resonances. This is consistent with a C_{2v}-symmetric structure in solution. Two resonances that integrate to 12H at δ 11.50 and 12.25 ppm can be assigned to two sets of isopropyl methyl groups. Further evidence of the ligand coordination can be observed from two other resonances that integrate to 4H at δ −60.16 and 56.44 ppm; both of these resonances are consistent with the alkyl-ether backbone of the ligand, although it is not possible to assign the two resonances to a particular methylene in the OCH$_2$CH$_2$N backbone. The remaining five ligand-related resonances all integrate to 2H and could not be further assigned. There is also one very broad resonance that integrates to 9H and is consistent with the presence of only one *tert*-butoxide group on the metal center.

Lactide Polymerization. Upon developing this series of new diamido-based actinide alkoxide complexes, we sought to determine their ability as initiators/catalysts for the ROP of lactide. Thus, the performance of the aforementioned complexes **1**−**5** and that of the previously reported dialkyl complexes [$^{t\mathrm{Bu}}$NON]An(CH$_2$SiMe$_3$)$_2$ (An = Th (**6**), U (**7**))[12a] and [$^{i\mathrm{Pr_2Ph}}$NCOCN]An(CH$_2$SiMe$_3$)$_2$ (An = Th (**8**), U (**9**))[11c,13] (Chart 1) in the ROP of L- and *rac*-lactide were assessed. The systematic use of different diamido ligands and different alkoxide ligands gives the opportunity to compare reactivities among the choice of amido-R group and ligand backbone, the choice of actinide metal, and the choice of alkoxide versus alkyl reactive group.

The results presented in Table 1 indicate that complexes **1**−**8** are all active initiators for the ROP of L-LA in toluene solution under ambient conditions, affording moderate to good control over the polymerization parameters; only **9** proved repeatedly inactive under the chosen experimental conditions. In almost all cases (except complexes **4** and **5** in entries 6 and 8), nearly complete conversion of 50 equiv of monomer was observed in less than 1 h. The distribution of the molecular weights remained monodispersed but spanned across a somewhat broad range, with values of M_w/M_n typically in the range 1.1−1.6. No clear relationship emerged from the comparison between the theoretical (calculated under the hypothesis of growth of a single PLLA chain per metal center) and calculated molecular weights.[15] Complexes **2**, **4**, and **7** stood out and gave generally a good agreement between these two values; this was accompanied by narrow molecular weight distributions expected for a well-behaved ROP initiator (Table 1, entries 2 and 3, 6 and 7, and 10 and 11). The control proved less efficient, however, when larger loadings of monomer were used (500 equiv, entries 4 and 12); the decreased M_n values (as compared to those obtained with 200 equiv) and the broader polydispersities likely call for transesterification and/or transfer-to-monomer side reactions under these conditions. Overall, the influence of the identity of the alkoxo initiating group (^{t}BuO$^-$ vs. ^{i}PrO$^-$) on the final outcome of the polymerization could not be rationalized; compare, for instance, entries 2, 5, and 6 in Table 1. Note, however, that perhaps unsurprisingly the "ate" complex **1** generally led to fast but poorly controlled reactions (entry 1).

Generally, the reactivities of complexes supported by the [$^{t\mathrm{Bu}}$NON]$^{2-}$ ligand are higher than those of complexes supported by the [$^{i\mathrm{Pr_2Ph}}$NCOCN]$^{2-}$ ligand. Complex **2** thus offered the best compromise between reaction rates and control over the ROP parameters. In particular, reactions catalyzed by **2** continued to exhibit high conversions and are adequately controlled (M_n(calcd) ≈ M_n(SEC); M_w/M_n = 1.26) even in the presence of 200 equiv of L-LA (Table 1, entry 3); at higher monomer loading (500 equiv), good conversions were still observed within a reasonably short time (90 min) but, as mentioned above, the molecular weight distributions increased noticeably (M_w/M_n = 1.54, entry 4). The ^{1}H NMR spectra of the polymers produced by **1** and **2** contain resonances that are in full agreement with the exclusive presence of both the ^{i}PrOC(═O)CH(CH$_3$)− and −CH(CH$_3$)OH end groups; no indication for the presence of diamido-ether moieties at the end

dx.doi.org/10.1021/om300993r | *Organometallics* 2013, 32, 1183−1192

Table 1. Ring-Opening Polymerization of L-LA Promoted by Complexes 1−9[a]

entry	compd	$[\text{L-LA}]_0/[\text{An}]_0$	time[b] (min)	conversn[c] (%)	M_n(calcd)[d] (g mol^{-1})	M_n(SEC)[e] (g mol^{-1})	M_w/M_n[e]
1	**1**	50	120	95	7000	9000	1.63[f]
2	**2**	50	30	86	6300	7700	1.16
3	**2**	200	60	91	26300	28900	1.26
4	**2**	500	90	69	65000	25700	1.54
5	**3**	50	30	47	3500	8000	1.50
6	**4**	50	30	14	1100	4500	1.24
7	**4**	50	120	100	7300	6800	1.15
8	**5**	50	30	17	1400	9800	1.49[f]
9	**6**	50	30	86	6300	29000	2.16
10	**7**	50	30	94	6900	11100	1.12
11	**7**	200	60	89	25800	35000	1.12
12	**7**	500	90	87	62800	29900	1.59
13	**8**	50	30	79	5800	14800	1.91[f]
14	**9**	50	30	<1	n/a	n/a	n/a

[a]Conditions: 1.0 M solution of L-LA in toluene, 30 °C. [b]The reaction time was not optimized. [c]Isolated yield after reprecipitation. [d]Calculated from M_n(calcd) = (144.13 × ($[\text{L-LA}]_0/[\text{An}]_0$) × conversion) + M_n(ROH) (ROH = ^{t}BuOH, ^{i}PrOH), for 1 PLLA chain per metal center. [e]M_n (g mol^{-1}) determined by SEC-RI against polystyrene standards and corrected by a factor of 0.58. [f]SEC analysis indicated a bimodal distribution.

of the polymer chains was ever observed. This is consistent with a coordination−insertion ROP scenario where initiation results from acyl cleavage following nucleophilic attack of only the isopropoxide group (and not the amido ligand $[^{t\text{Bu}}\text{NON}]^{2-}$) on the coordinated monomer and subsequent opening of the heterocycle. Similarly the ^{1}H NMR spectra of polymers produced by complexes **3**−**5** have resonances that are consistent with ^{t}BuOC(=O)CH(CH_3)− and −CH(CH_3)OH end groups; again, there was no evidence in the NMR spectra to suggest that the actinide catalyst decomposed under ROP conditions or that the diamido-ether ancillary ligand, be it $[^{i\text{Pr}_2\text{Ph}}\text{NCOCN}]^{2-}$ or $[^{t\text{Bu}}\text{NON}]^{2-}$, acts as an initiating group in these ROP reactions.

We sought to investigate the reaction kinetics with these diamido actinide catalysts via in situ monitoring of a ROP reaction by ^{1}H NMR spectroscopy. Ideally, **2** would be the best candidate for these kinetic measurements because it exhibits a well-controlled polymerization behavior and enables the ROP of monomer loadings suited to NMR-scale reactions. However, **2** (Table 1, entries 2−4) completely converts 50−200 equiv of L-LA in less than 1 h, and while this is desirable for an active initiator, it makes NMR monitoring more difficult, and a slower catalyst would be easier to follow. Furthermore, **2** is paramagnetic, which precludes accurate NMR monitoring of ROP reactions. Complex **1** (the available diamagnetic complex most similar to **2** since it contains the same ancillary ligand and reactive nucleophile, $[^{t\text{Bu}}\text{NON}]^{2-}$ and ^{i}PrO$^-$, respectively) was not selected because it only afforded poorly controlled ROP reactions. Instead, the reaction kinetics of **4** were examined, since this compound demonstrated similar control over the polymerization to **2** (Table 1, entries 2 and 7), is diamagnetic, and takes somewhat longer than **2** to reach full conversion of 50 equiv of monomer, making it more compatible for NMR monitoring. Figure 3 contains a plot of monomer conversion vs reaction time for the ROP of L-LA catalyzed by **4** in toluene-d_8 under ambient conditions. A short induction period was observed; the reaction followed partial first-order kinetics with respect to monomer concentration, and the value k_{app} = 0.408 × 10^{-3} s^{-1} was extracted from the semilogarithmic plot of monomer conversion vs reaction time (Supporting Information).

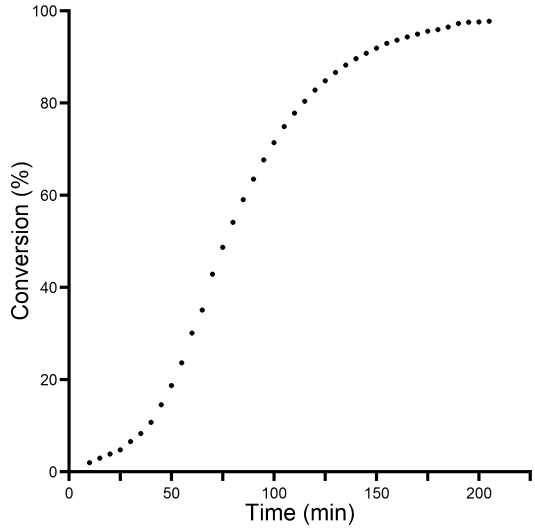

Figure 3. Plot of monomer conversion vs reaction time for the ROP of L-LA catalyzed by **4**, with [L-LA]/[**4**] = 50/1, $[\text{L-LA}]_0$ = 1.0 M in toluene-d_8, and 30 °C.

The bottom half of Table 1 pertains to the ROP of L-LA catalyzed by the previously reported diamido dialkyl complexes **6**−**9**. Unlike the related alkoxide complexes **1** and **2**, the dialkyls **6**−**9** portray a wider range of control over polymerization. The uranium-based **7**, $[^{t\text{Bu}}\text{NON}]\text{U}(\text{CH}_2\text{SiMe}_3)_2$, notably afforded the best control of all four dialkyl complexes (entries 10−12). The thorium dialkyls **6** and **8** gave PLLAs presenting a broad polydispersity, while the second uranium complex, **9**, did not promote any polymerization over the allotted time period, forming instead amorphous oils that could not be characterized. End-group analysis of a PLLA sample produced from **7** was performed via NMR spectroscopy, in an effort to determine which of the alkyl or diamido ligands acts as the initiating group in these ROP. The ^{1}H, ^{13}C{^{1}H}, and 2D (HMBC, HMQC) NMR analyses confirmed that the alkyl group Me_3SiCH_2− does initiate the polymerization; no evidence for an amide-based end group was detected. In addition, the combined NMR data indicate that the −C(=O)CH_2SiMe_3 group at the polymer chain end did not remain intact following quenching of the reaction with acidified

dx.doi.org/10.1021/om300993r | Organometallics 2013, 32, 1183−1192

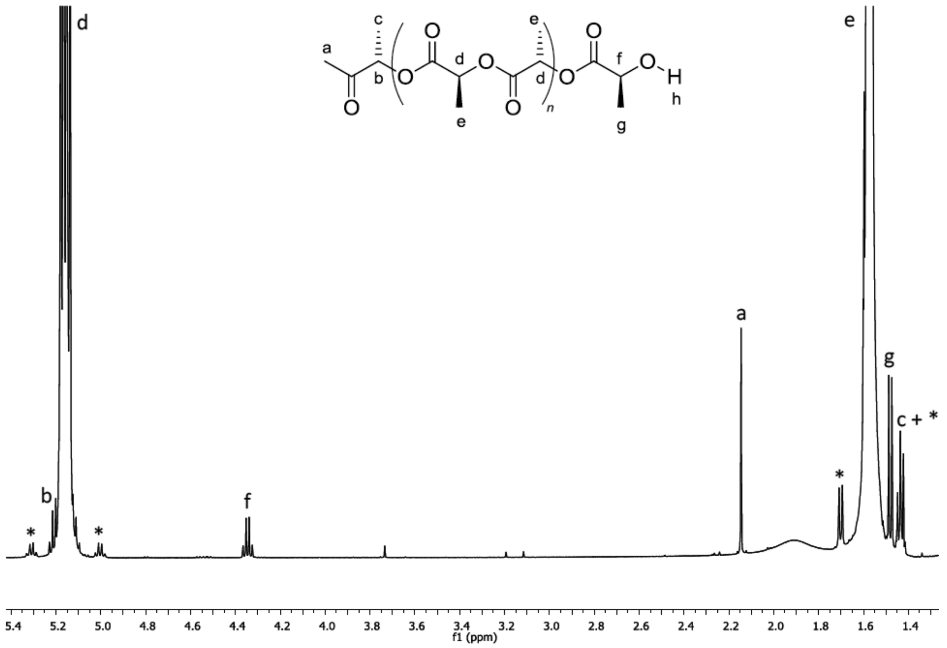

Figure 4. ^{1}H NMR spectrum (500.13 MHz, chloroform-*d*, 298 K) of a $CH_3C(=O)-$ terminated PLLA prepared with **7** (Table 1, entry 10). Asterisks denote ^{13}C satellites associated with resonances d and e.

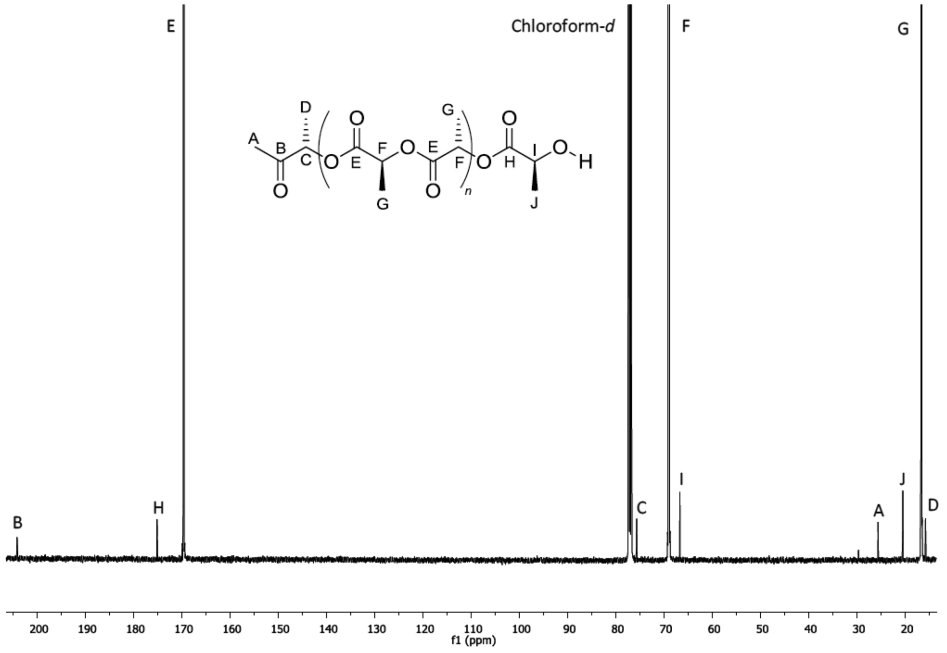

Figure 5. $^{13}C\{^{1}H\}$ NMR spectrum (chloroform-*d*, 125.78 MHz, 298 K) of a $CH_3C(=O)-$ terminated PLLA prepared with **7** (Table 1, entry 10).

methanol and complete workup. Instead, the $C(=O)CH_2-SiMe_3$ bond was quantitatively hydrolyzed and a methyl ketone group, $-C(=O)CH_3$, solely remained as this end of the polymer chain (Figures 4 and 5),[16] together with $-CH(CH_3)$-OH as the opposite end group. Complete, corroborative NMR analysis is provided in the Supporting Information. To further confirm this interpretation, the same PLLA sample was further analyzed by MALDI-TOF mass spectrometry. The mass spectrum shows the presence of a major population of chains terminated by a $CH_3C(=O)CH(CH_3)-$ fragment, with increments of 72 Da between consecutive peaks corresponding to half a L-LA unit; these data were diagnostic of extended transesterification side reactions (if transesterification would have not occurred, only lactide repeat units would be observed (i.e., 144 Da increments)) and provided additional evidence for the proposed composition of the PLLA chains, namely $CH_3C(=O)CH(CH_3)[O(C(=O)CH(CH_3)]_nOC(=O)CH(CH_3)OH$. Although a number of reports of alkyl end-capped polylactides can be found in the literature,[17] these prior characterizations are incomplete and we therefore believe this is the first time that ROP initiation by a $-CH_2SiMe_3$ moiety leading to the formation of PLLA chains has been unambiguously evidenced.

Complex **2**, the most competent ROP initiator in the series of actinide complexes **1**–**9**, was employed for additional studies involving *rac*-LA, the results of which are summarized in Table

dx.doi.org/10.1021/om300993r | *Organometallics* 2013, 32, 1183–1192

Table 2. ROP of *rac*-LA with 2[a]

entry	solvent	time[b] (h)	conversn[c] (%)	M_n(calcd)[d] (g mol^{-1})	M_n(SEC)[e] (g mol^{-1})	M_w/M_n[e]	P_r
1	Tol	2	68	5000	9600	1.24	0.61
2	THF	2	49	3600	5200	1.25	0.73

[a]Conditions: [*rac*-LA]$_0$ = 1.0 M, [*rac*-LA]$_0$/[**2**]$_0$ = 50/1, 30 °C. [b]The reaction time was not optimized. [c]Conversion determined by ^{1}H NMR. [d]Calculated from M_n(calcd) = (144.13 × ([*rac*-LA]$_0$/[**2**]$_0$) × conversion) + 62.10. [e]M_n (g mol^{-1}) determined by SEC-RI against polystyrene standards and corrected by a factor of 0.58.

2. The ROP reactions were relatively well controlled in toluene with relatively low polydispersity values (M_w/M_n = 1.24), but we found that in this case the reaction proceeded more slowly than previously with the enantiopure L-LA. The homonuclear decoupled ^{1}H NMR spectrum of PLA produced with **2** in toluene indicates a polymer with an estimated P_r value of 0.61 (entry 1), indicating a slight tendency toward heterotacticity. This value was increased by changing the solvent to THF (entry 2), with an estimated P_r value of 0.73, diagnostic of a more significant heterotactic enrichment. This improvement in stereocontrol, however, came at the expense of reaction rates, likely attributable to competitive coordination of THF onto the metal center. Lowering the temperature to 5 °C resulted in poor yields after 4−12 h for no benefit in terms of stereoselectivity, and efforts to maximize catalytic activity were therefore not pursued; note that high conversions were observed when the reaction time was extended to 24 or 48 h at this temperature, but the resulting materials consisted of intractable oils (probably as a result of excessive deleterious transesterification side reactions over the prolonged reaction times) which we failed to characterize adequately.

CONCLUSIONS

Diamido-ether actinide alkoxide complexes **1**−**5** were prepared in good to high yields from the corresponding diamido actinide halide complexes and were characterized. Complex **1** is an "ate" complex, while compounds **2**−**5** are salt and solvent free. Complexes **1**−**5** and the diamido actinide dialkyls **6**−**9** were evaluated as initiators for the ROP of L-LA. It was determined that complexes **1**−**8** were active for the polymerization of 50 equiv of monomer at room temperature. Except for complexes **4** and **5**, the reaction reaches completion in less than 1 h. This represents the first report of heteroleptic amide actinide alkoxide complexes capable of facilitating this reaction and is also in fact one of only a few reports of actinide-based catalysts that have been used for this reaction. Analysis of the polymers synthesized by **1**−**8** indicated a range of control over the polymerizations where generally the uranium complexes exhibited the best control over the polymerization parameters. End-group analyses of the polymers showed that the diamido ligands do not participate as initiating groups in the polymerization; moreover, examination of PLLAs prepared by dialkyl complexes **6**−**8** demonstrated initiation by the alkyl moiety in these initiators. Complex **2** was also evaluated for the ROP of *rac*-lactide. The PLAs obtained using *rac*-lactide displayed a propensity toward heterotacticity, with a P_r value up to 0.73 in THF.

EXPERIMENTAL SECTION

General Considerations. All techniques and procedures were carried out under a nitrogen atmosphere either with an Mbraun Labmaster 130 glovebox or using standard Schlenk and vacuum-line techniques. All glassware was dried overnight at 160 °C prior to use. Toluene, tetrahydrofuran (THF), and diethyl ether were distilled from a sodium/benzophenone solution under nitrogen. Hexanes were distilled from a sodium solution under nitrogen. Deuterated solvents were distilled from a sodium/benzophenone solution. UCl_4,[18] $ThCl_4$·2DME,[19] (^{t}BuNH(SiMe$_2$))$_2$O ([^{tBu}NON]H$_2$),[20] (2,6-^{i}Pr$_2$PhNH(CH$_2$CH$_2$))$_2$O ([^{iPr_2Ph}NCOCN]H$_2$),[21] {[^{tBu}NON]-UCl$_2$}$_2$,[12a] [^{tBu}NON]ThCl$_5$Li$_3$·DME,[11c] [^{iPr_2Ph}NCOCN]-UCl$_3$Li·2THF,[13] [^{iPr_2Ph}NCOCN]ThCl$_2$·DME,[11c] [^{tBu}NON]U-(CH$_2$SiMe$_3$)$_2$,[12a] [^{tBu}NON]Th(CH$_2$SiMe$_3$)$_2$,[11c,12a] [^{iPr_2Ph}NCOCN]U-(CH$_2$SiMe$_3$)$_2$,[13] and [^{iPr_2Ph}NCOCN]Th(CH$_2$SiMe$_3$)$_2$[11c] were prepared in accordance with published literature procedures. L-lactide and *rac*-lactide were purified by recrystallization once from *iso*-propanol and twice more from anhydrous toluene, then dried *in vacuo*. All other reagents were purchased from commercial sources and used without further purification.

NMR spectra were recorded at 294 K, unless otherwise stated, on a 400 MHz Bruker Avance III spectrometer, a 500 MHz Bruker Avance III spectrometer, or a 600 MHz Bruker Avance II spectrometer with a 5 mm QNP cryoprobe. ^{1}H and ^{13}C NMR shifts are reported in ppm relative to residual solvent resonances: specifically for ^{1}H, benzene-d_6 at δ 7.15 or toluene-d_8 at δ_{Me} 2.06 ppm, and for ^{13}C, benzene-d_6 at δ 128.06 or toluene-d_8 at δ_{Me} 20.43 ppm. Elemental analyses (C, H, N) were performed at Simon Fraser University by Mr. Farzad Haftbaradaran employing a Carlo Erba EA 1110 CHN elemental analyzer. Size exclusion chromatography (SEC) analyses of PLAs were performed on a Polymer Laboratories PL-GPC 50 instrument equipped with two PLgel 5 Å MIXED-C columns and a refractive index detector. The column was eluted with THF at room temperature at 1.0 mL min^{-1} and was calibrated using 11 monodisperse polystyrene standards in the range of 580−380000 g mol^{-1}. The molecular weights of all PLAs were corrected by a factor of 0.58. MALDI-TOF mass spectra of PLAs were obtained with a Bruker Daltonic MicroFlex LT apparatus, using a nitrogen laser source (337 nm, 3 ns) in linear mode with a positive acceleration voltage of 20 kV. Samples were prepared as follows: 1 μL of a 2/1 mixture of a saturated solution of α-cyano-4-hydroxycinnamic acid (Bruker Care) in HPLC-quality acetonitrile and a 0.1% solution of trifluoroacetic acid in ultrapure water were deposited on the sample plate. After total evaporation, 1 μL of a 5−10 mg mL^{-1} solution of the polymers in HPLC-quality THF was deposited. Bruker Care Peptide Calibration Standard and Protein Calibration Standard I were used for external calibration.

[^{tBu}NON]Th(O^{i}Pr)$_3$Li·Solv (1-solv). [^{tBu}NON]ThCl$_2$·DME (0.100 g, 0.17 mmol) was dissolved in toluene (20 mL), and 3 equiv of LiO^{i}Pr (0.52 mL, 0.52 mmol) dissolved in toluene (20 mL) was added dropwise via syringe at room temperature. Upon addition the reaction became cloudy and pale yellow. Stirring was continued at room temperature for 18 h, after which the reaction was filtered through a Celite-padded medium-porosity glass frit, resulting in a clear, pale yellow solution. Excess toluene was removed *in vacuo* to yield a beige-yellow solid of [^{tBu}NON]Th(O^{i}Pr)$_3$Li·DME (**1-DME**; 0.106 g, 79%). Crystals suitable for X-ray diffraction were grown by slow evaporation of a toluene/diethyl ether solution (**1-Et$_2$O**) at room temperature. Anal. Calcd for $C_{25}H_{61}LiN_2O_6Si_2Th$: C, 38.45; H, 7.87; N, 3.59. Found: C, 38.65; H, 7.71; N, 3.57. ^{1}H NMR (toluene-d_8, 500 MHz, 298 K): δ 0.44 (s, 6H, Si(CH_3)$_2$), 0.50 (s, 6H, Si(CH_3)$_2$), 1.26 (d, ^3J = 7.5 Hz, 12H, OCH(CH_3)$_2$), 1.41−1.50 (overlapping signals, d, 6H, CH(CH_3)$_2$ and s, 18H, C(CH_3)$_3$), 2.81 (s, 4H, OCH_2, DME), 3.04 (s, 6H, OCH_3, DME), 4.59 (br m, 2H, CH(CH$_3$)$_2$), 4.66 (sept, ^3J = 7.5 Hz, 1H, CH(CH$_3$)$_2$). ^{1}H NMR (toluene-d_8, 400 MHz, 233 K): δ 0.50 (s, 6H, Si(CH_3)$_2$), 0.54 (s, 6H, Si(CH_3)$_2$), 1.2−1.3 (vv br s, 12H, CH(CH_3)$_2$), 1.52−1.54 (overlapping signals, 24H, d, CH(CH_3)$_2$, and

dx.doi.org/10.1021/om300993r | *Organometallics* 2013, 32, 1183−1192

s, C(CH_3)$_3$), 2.50 (s, 4H, OCH_2, DME), 2.88 (s, 6H, OCH_3, DME), 4.5 (v br s, 2H, CH(CH$_3$)$_2$), 4.61 (br s, 1H, CH(CH$_3$)$_2$). ^{1}H NMR (toluene-d_8, 400 MHz, 193 K): δ 0.54 (s, 6H, Si(CH_3)$_2$), 0.58 (s, 6H, Si(CH_3)$_2$), 1.21 (s, 6H, CH(CH_3)$_2$), 1.30 (s, 6H, CH(CH_3)$_2$), 1.58 (s, *ca.* 18H, C(CH_3)$_3$), 1.58−1.65 (v br sh, *ca.* 6H, CH(CH_3)$_2$), 2.32 (s, 4H, OCH_2, DME), 2.78 (s, 6H, OCH_3, DME), 4.61 (br s, 1H, CH(CH$_3$)$_2$), 4.69 (br s, 1H, CH(CH$_3$)$_2$), 4.87 (s, 1H, CH(CH$_3$)$_2$). ^{13}C{^{1}H} NMR (toluene-d_8, 125 MHz, 298 K): δ 6.91 (Si(CH_3)$_2$), 6.94 (Si(CH_3)$_2$), 28.80 (CH(CH_3)$_2$), 28.99 (C(CH_3)$_3$), 35.81 (CH-(CH_3)$_2$), 58.92 (O−CH_3, DME), 66.42 (CH(CH$_3$)$_2$), 70.03 (O−CH_2, DME), 72.58 (CH(CH$_3$)$_2$).

{[^{tBu}NON]U(O^{i}Pr)$_2$}$_2$ (2). {[^{tBu}NON]UCl$_2$}$_2$ (0.100 g, 0.171 mmol) was dissolved in toluene (20 mL), and 2 equiv of LiO^{i}Pr (0.34 mL, 0.343 mmol) dissolved in toluene (20 mL) was added dropwise via syringe at room temperature. Upon addition the reaction mixture turned golden brown. Stirring was continued at room temperature for 18 h, after which the reaction mixture was filtered through a Celite-padded medium-porosity glass frit, resulting in a clear yellow-brown solution. Excess toluene was removed *in vacuo* to yield a brown solid of {[^{tBu}NON]U(O^{i}Pr)$_2$}$_2$ (**2**; 0.233 g, 93%). Crystals suitable for X-ray diffraction were grown by slow evaporation of a toluene solution at room temperature. Anal. Calcd for $C_{18}H_{44}N_2O_3Si_2U$: C, 34.28; H, 7.03; N, 4.44. Found: C, 33.95; H, 6.63; N, 4.24. ^{1}H NMR (benzene-d_6, 400 MHz, 298 K): δ 100.18 (br, 6H), 77.90 (1H, OCH(CH$_3$)$_2$), 41.47 (br, 6H), −16.24 (1H, OCH(CH$_3$)$_2$), −24.72 (br, 6H), −31.45 (br, 6H), −49.55 (br, 18H, NC(CH_3)$_3$).

[^{tBu}NON]U(O^{t}Bu)$_2$ (3). {[^{tBu}NON]UCl$_2$}$_2$ (0.100 g, 0.171 mmol) was dissolved in toluene (20 mL), and 2 equiv of KO^{t}Bu (0.038 g, 0.343 mmol) suspended in toluene (20 mL) was added slowly at room temperature. Within 5 min of addition the reaction mixture turned light brown. Stirring was continued for 18 h at room temperature without any further changes, after which the reaction was filtered through a Celite-padded medium-porosity glass frit, resulting in a clear red-brown solution. Excess toluene was removed *in vacuo* to give a red-brown solid of [^{tBu}NON]U(O^{t}Bu)$_2$ (**3**; 0.101 g, 89%). Anal. Calcd for $C_{45}H_{108}N_4O_6Si_4U_2$: C, 38.89; H, 7.83; N, 4.03. Found: C, 39.20; H, 7.81; N, 3.47. ^{1}H NMR (benzene-d_6, 400 MHz, 298 K): δ −44.57 (6H, Si(CH_3)$_2$), −42.51 (6H, Si(CH_3)$_2$), −37.55 (v br, 18H), −10.07 (v br, 18H).

[^{iPr_2Ph}NCOCN]Th(O^{t}Bu)$_2$ (4). [^{iPr_2Ph}NCOCN]ThCl$_2$·DME (0.200 g, 0.245 mmol) was dissolved in DME, and 2 equiv of KO^{t}Bu (0.055 g, 0.490 mmol) dissolved in DME was added slowly at room temperature. The reaction mixture immediately turned a cloudy orange-brown. Stirring was continued for 24 h at room temperature, after which the reaction was filtered through a Celite-padded medium-porosity glass frit, resulting in a clear light orange solution. Excess DME was removed *in vacuo* to give an orange solid of [^{iPr_2Ph}NCOCN]-Th(O^{t}Bu)$_2$ (**4**; 0.155 g, 79%). Anal. Calcd for $C_{36}H_{60}N_2O_3Th$: C, 53.99; H, 7.55; N, 3.50. Found: C, 53.17; H, 7.24; N, 3.34 (the values are all slightly low, most likely because a small amount (less than 0.25 equiv) of KCl cannot be separated from the compound due to their very similar solubilities). ^{1}H NMR (toluene-d_8, 600 MHz, 298 K): δ 1.09 (br s, 18H, OC(CH_3)$_3$), 1.27 (d, ^3J = 10.2 Hz, 24H, N−Ar−CH(CH_3)$_2$), 3.44 (t, ^3J = 7.8 Hz, 4H, NCH_2CH$_2$O), 3.70 (sept, ^3J = 10.2 Hz, 4H, N−Ar−CH(CH$_3$)$_2$), 3.80 (t, ^3J = 9.6 Hz, 4H, NCH$_2$CH_2O), 7.09−7.13 (m, 12 H, N-*Ar*). ^{13}C{^{1}H} NMR (toluene-d_8, 150 MHz, 298 K): δ 14.32 (N−Ar−CH(CH_3)$_2$), 22.75 (OC(CH_3)$_3$), 24.53 (N−Ar-CH(CH_3)$_2$), 27.89 (OC(CH_3)$_3$), 33.27 (NCH$_2$CH$_2$O), 34.44 (NCH_2CH$_2$O), 124.03 (Ar−*C*), 124.48 (Ar−*C*), 142.90 (N−Ar−C$_{ipso}$).

[^{iPr_2Ph}NCOCN]U(O^{t}Bu)Cl (5). [^{iPr_2Ph}NCOCN]UCl$_3$Li·THF (0.190 g, 0.260 mmol) was dissolved in toluene (20 mL), and 1 equiv of KO^{t}Bu (0.029 g, 0.260 mmol) suspended in toluene (20 mL) was added slowly at room temperature. The reaction mixture immediately turned dark red brown. Stirring was continued for 24 h at room temperature, after which the reaction mixture was filtered through a Celite-padded medium-porosity glass frit, resulting in a clear red-brown solution. Excess toluene was removed *in vacuo* to give a brown solid of [^{iPr_2Ph}NCOCN]U(O^{t}Bu)Cl (**5**; 0.180 g, 90%). Anal. Calcd for $C_{32}H_{51}N_2O_2ClU$: C, 49.96; H, 6.68; N, 3.64. Found: C, 50.10; H, 6.70; N, 3.76. ^{1}H NMR (toluene-d_8, 400 MHz, 298 K): δ −78.97 (2H), −72.85 (2H), −67.99 (2H), −60.16 (4H, NCH$_2$CH$_2$O), 1.08 (v br, 9H, OC(CH_3)$_3$), 11.50 (12H, N−Ar−CH(CH_3)$_2$), 12.25 (12H, N−Ar−CH(CH_3)$_2$), 45.99 (2H), 56.44 (4H, NCH$_2$CH$_2$O), 59.73 (2H).

Lactide Polymerization. In a typical polymerization procedure (Table 1, entry 1), a 30 mL Schlenk flask was charged with 0.015 g of **1** (or another compound, as appropriate) and 50 equiv of L-lactide (0.139 g). The two compounds were dissolved in 1.8 mL of toluene to give a 1.0 M solution of lactide. The reaction mixture was placed in an oil bath heated to 30 °C for the specified time (usually 30 min) with magnetic stirring. After the desired time, the reaction was quenched via the addition of a few drops of a 3% HCl/MeOH solution and the polymer was precipitated as a white solid through the addition of excess MeOH. The solid precipitate was collected via filtration and dried overnight *in vacuo* to a constant weight.

X-ray Crystallography. Crystallographic data for **1·Et$_2$O** and **2** are collected in Table 3. Both crystals were coated in Paratone oil, mounted on a MiTeGen Micro Mount, and transferred to the cold stream (150 K) of the X-ray diffractometer. Crystal descriptions for each compound are as follows: **1·Et$_2$O** was a clear, colorless rectangular plate and **2** was a brown-green arrowhead-shaped plate. Both crystals, while they diffracted strongly, were not of high quality (mild twinning etc.), and despite multiple efforts to prepare good crystals, the final *R* values reflect this circumstance. All data were collected on a Bruker Smart instrument equipped with an APEX II CCD area detector fixed at a distance of 6.0 cm from the crystal and a Mo Kα fine-focus sealed tube (λ = 0.71073 nm) operated at 1.5 kW (50 kV, 30 mA) and filtered with a graphite monochromator. The temperature was regulated using an Oxford Cryosystems Cryostream; both crystals were collected at 150 K. Data reduction and absorption correction details can be found in the Supporting Information.

The structures were solved using direct methods (SIR 92) and refined by least-squares procedures using CRYSTALS.[22] Hydrogen atoms on carbon atoms were included at the geometrically idealized positions (C−H bond distance 0.95 Å) and were not refined. The isotropic thermal parameters of the hydrogen atoms were fixed at 1.2 times that of the preceding carbon atom. The plots for the crystal structures were generated using ORTEP-3 for windows (v. 2.00)[23] and rendered using POV-Ray (v. 3.6.1).[24] Thermal ellipsoids are shown at the 30% probability level.

Table 3. Summary of Crystallographic Data

	1·Et$_2$O	**2**
formula	$C_{50}H_{119}Li_2N_4O_{10}Si_4Th_2$	$C_{36}H_{88}N_4O_6Si_4U_2$
M_w/g mol^{-1}	1526.81	1261.52
cryst dimens/mm	0.13 × 0.10 × 0.10	0.35 × 0.15 × 0.10
cryst syst	orthorhombic	orthorhombic
space group	*Pnam*	*Cmca*
T/K	150	150
a/Å	26.4650(19)	17.5704(19)
b/Å	11.1898(8)	12.6855(14)
c/Å	12.9222(9)	22.676(3)
α/deg	90	90
β/deg	90	90
γ/deg	90	90
V/Å^3	3826.8(5)	5054.2(10)
Z	2	4
D_c/g cm^{-3}	1.328	1.658
μ/cm^{-1}	3.988	6.536
R ($I > 2.5\sigma(I)$)[a]	0.0760	0.0983
R_w ($I > 2.5\sigma(I)$)[a]	0.0742	0.0728
GOF	3.5262	5.4911

[a]The function minimized was $\sum w(|F_o| - |F_c|)^2$, where $w^{-1} = [\sigma^2(F_o) + (nF_o)^2]$ with n = 0.01 for **1·Et$_2$O** and 0.00 for **2**. $R = \sum||F_o| - |F_c||/\sum|F_o|$; $R_w = [\sum w(|F_o| - |F_c|)^2/\sum w|F_o|^2]^{1/2}$.

For **1·Et$_2$O** and **2** the coordinates and anisotropic displacement parameters for all non-hydrogen atoms were refined, with the exception of the terminally bound O^{i}Pr group for both crystals, one of the bridging O^{i}Pr groups in **1·Et$_2$O**, and the ether molecule in **1·Et$_2$O**. These O^{i}Pr groups were found to be rotationally disordered in all three cases and were treated accordingly. The ether molecule was also found to be disordered over two positions and was treated accordingly; the larger of the two components of the disorder is shown in Figure 1.

■ ASSOCIATED CONTENT

Supporting Information

CIF files and figures giving complete crystallographic data for all reported crystal structures and ^{1}H and ^{13}C NMR spectra of the diamagnetic complexes, as well as representative NMR and mass spectra of some polymers. This material is available free of charge via the Internet at http://pubs.acs.org.

■ AUTHOR INFORMATION

Corresponding Author

*D.B.L: tel, 1-778-782-4887; fax, 1-778-782-3765; e-mail, dleznoff@sfu.ca. J.-F.C.: tel, 33-223-235-950; fax, 33-223-236-939; e-mail, jean-francois.carpentier@univ-rennes1.fr.

Notes

The authors declare no competing financial interest.

■ ACKNOWLEDGMENTS

This work was supported by the NSERC of Canada and CNRS of France. C.E.H. is grateful to the NSERC for a Doctoral Post-Graduate Scholarship.

■ REFERENCES

(1) (a) O'Keefe, B. J.; Hillmyer, M. A.; Tolman, W. B. *Dalton Trans.* **2001**, 2215. (b) Dechy-Cabaret, O.; Martin-Vaca, B.; Bourissou, D. *Chem. Rev.* **2004**, *104*, 6147. (c) Wheaton, C. A.; Hayes, P. G.; Ireland, B. J. *Dalton Trans.* **2009**, 4832. (d) Ajellal, N.; Carpentier, J.-F.; Guillaume, C.; Guillaume, S. M.; Héelou, M.; Poirier, V.; Sarazin, Y.; Trifonov, A. *Dalton Trans.* **2010**, *39*, 8363. (e) Carpentier, J.-F. *Macromol. Rapid Commun.* **2010**, *31*, 1696. (f) Stanford, M. J.; Dove, A. P. *Chem. Soc. Rev.* **2010**, *39*, 486. (g) Thomas, C. M. *Chem. Soc. Rev.* **2010**, *39*, 165. (h) Dijkstra, P. J.; Du, H.; Feijen, J. *Polymer Chemistry* **2011**, *2*, 520.

(2) (a) Bonnet, F.; Cowley, A. R.; Mountford, P. *Inorg. Chem.* **2005**, *44*, 9046. (b) Skvortsov, G. G.; Yakovenko, M. V.; Castro, P. M.; Fukin, G. K.; Cherkasov, A. V.; Carpentier, J.-F.; Trifonov, A. A. *Eur. J. Inorg. Chem.* **2007**, 3260. (c) Wang, J.; Cai, T.; Yao, Y.; Zhang, Y.; Shen, Q. *Dalton Trans.* **2007**, 5275. (d) Ajellal, N.; Lyubov, D. M.; Sinenkov, M. A.; Fukin, G. K.; Cherkasov, A. V.; Thomas, C. M.; Carpentier, J.-F.; Trifonov, A. A. *Chem. Eur. J.* **2008**, *14*, 5440. (e) Dyer, H. E.; Huijser, S.; Schwarz, A. D.; Wang, C.; Duchateau, R.; Mountford, P. *Dalton Trans.* **2008**, 32. (f) Dyer, H. E.; Huijser, S.; Susperregui, N.; Bonnet, F.; Schwarz, A. D.; Duchateau, R.; Maron, L.; Mountford, P. *Organometallics* **2010**, *29*, 3602. (g) Sinenkov, M.; Kirillov, E.; Roisnel, T.; Fukin, G.; Trifonov, A.; Carpentier, J.-F. *Organometallics* **2011**, *30*, 5509. (h) Li, W.; Xue, M.; Tu, J.; Zhang, Y.; Shen, Q. *Dalton Trans.* **2012**, *41*, 7258. (i) Zhang, X.; Wang, C.; Xue, M.; Zhang, Y.; Yao, Y.; Shen, Q. *J. Organomet. Chem.* **2012**, *713*, 182.

(3) (a) Cheng, M.; Attygalle, A. B.; Lobkovsky, E. B.; Coates, G. W. *J. Am. Chem. Soc.* **1999**, *121*, 11583. (b) Chamberlain, B. M.; Cheng, M.; Moore, D. R.; Ovitt, T. M.; Lobkovsky, E. B.; Coates, G. W. *J. Am. Chem. Soc.* **2001**, *123*, 3229. (c) Platel, R. H.; Hodgson, L. M.; White, A. J. P.; Williams, C. K. *Organometallics* **2007**, *26*, 4955. (d) Schwarz, A. D.; Thompson, A. L.; Mountford, P. *Inorg. Chem.* **2009**, *48*, 10442. (e) Schwarz, A. D.; Herbert, K. R.; Paniagua, C.; Mountford, P. *Organometallics* **2010**, *29*, 4171. (f) Platel, R. H.; White, A. J. P.; Williams, C. K. *Inorg. Chem.* **2011**, *50*, 7718.

(4) (a) Li, H.-X.; Xu, Q.-F.; Chen, J.-X.; Cheng, M.-L.; Zhang, Y.; Zhang, W.-H.; Lang, J.-P.; Shen, Q. *J. Organomet. Chem.* **2004**, *689*, 3438. (b) Heck, R.; Schulz, E.; Collin, J.; Carpentier, J.-F. *J. Mol. Catal. A* **2007**, *268*, 163. (c) Mahrova, T. V.; Fukin, G. K.; Cherkasov, A. V.; Trifonov, A. A.; Ajellal, N.; Carpentier, J.-F. *Inorg. Chem.* **2009**, *48*, 4258.

(5) (a) Barnea, E.; Moradove, D.; Berthet, J.-C.; Ephritikhine, M.; Eisen, M. S. *Organometallics* **2006**, *25*, 320. (b) Rabinovich, E.; Aharonovich, S.; Botoshansky, M.; Eisen, M. S. *Dalton Trans.* **2010**, *39*, 6667.

(6) (a) Katz, J. J.; Seaborg, G. T.; Morss, L. R. *The Chemistry of the Actinide Elements*; Chapman and Hall: New York, 1986. (b) Barnea, E.; Eisen, M. S. *Coord. Chem. Rev.* **2006**, *250*, 855. (c) Ephritikhine, M. *Dalton Trans.* **2006**, 2501. (d) Andrea, T.; Eisen, M. S. *Chem. Soc. Rev.* **2008**, *37*, 550.

(7) Berthet, J. C.; Ephritikhine, M. *Coord. Chem. Rev.* **1998**, *178–180*, 83.

(8) (a) Andrea, T.; Barnea, E.; Eisen, M. S. *J. Am. Chem. Soc.* **2008**, *130*, 2454. (b) Weiss, C. J.; Marks, T. J. *Dalton Trans.* **2010**, *39*, 6576. (c) Sharma, M.; Andrea, T.; Brookes, N. J.; Yates, B. F.; Eisen, M. S. *J. Am. Chem. Soc.* **2011**, *133*, 1341.

(9) (a) Cotton, F. A.; Marler, D. O.; Schwotzer, W. *Inorg. Chem.* **1984**, *23*, 4211. (b) Berg, J. M.; Clark, D. L.; Huffman, J. C.; Morris, D. E.; Sattelberger, A. P.; Streib, W. E.; Sluys, W. G. V. D.; Watkin, J. G. *J. Am. Chem. Soc.* **1992**, *114*, 10811. (c) Clark, D. L.; Huffman, J. C.; Watkin, J. G. *J. Chem. Soc., Dalton Trans.* **1992**, 266. (d) Clark, D. L.; Watkin, J. G. *Inorg. Chem.* **1993**, *32*, 1766. (e) Avens, L. R.; Barnhart, D. M.; Burns, C. J.; McKee, S. D.; Smith, W. H. *Inorg. Chem.* **1994**, *33*, 4245. (f) Barnhart, D. M.; Clark, D. L.; Grumbine, S. K.; Watkin, J. G. *Inorg. Chem.* **1994**, *34*, 1695. (g) Fortier, S.; Wu, G.; Hayton, T. W. *Inorg. Chem.* **2008**, *47*, 4752. (h) Mansell, S. M.; Kaltsoyannis, N.; Arnold, P. L. *J. Am. Chem. Soc.* **2011**, *133*, 9036. (i) Marciniec, B.; Maciejewski, H. *Coord. Chem. Rev.* **2001**, *223*, 301.

(10) (a) Bruno, J. W.; Stecher, H. A.; Morss, L. R.; Sonnenberger, D. C.; Marks, T. J. *J. Am. Chem. Soc.* **1986**, *108*, 7275. (b) Lin, Z.; Marks, T. J. *J. Am. Chem. Soc.* **1990**, *112*, 5515. (c) Scott, P.; Hitchcock, P. B. *J. Chem. Soc., Dalton Trans.* **1995**, 603. (d) Butcher, R. J.; Clark, D. L.; Grumbine, S. K.; Scott, B. L.; Watkin, J. G. *Organometallics* **1996**, *15*, 1488. (e) Roussel, P.; Hitchcock, P. B.; Tinker, N. D.; Scott, P. *Inorg. Chem.* **1997**, *36*, 5716. (f) Karmazin, L.; Mazzanti, M.; Pecaut, J. *Inorg. Chem.* **2003**, *42*, 5900. (g) Castro-Rodriguez, I.; Nakai, H.; Zakharov, L. N.; Rheingold, A. L.; Meyer, K. *Science* **2004**, *305*, 1757. (h) Arnold, P. L.; Liddle, S. T. *Chem. Commun.* **2006**, 3959. (i) Andrea, T.; Barnea, E.; Botoshansky, M.; Kapon, M.; Genizi, E.; Goldschmidt, Z.; Eisen, M. S. *J. Organomet. Chem.* **2007**, *692*, 1074. (j) Stubbert, B. D.; Marks, T. J. *J. Am. Chem. Soc.* **2007**, *129*, 6149. (k) Masuda, J. D.; Jantunen, K. C.; Scott, B. L.; Kiplinger, J. L. *Organometallics* **2008**, *27*, 1299. (l) Bart, S. C.; Heinemann, F. W.; Anthon, C.; Hauser, C.; Meyer, K. *Inorg. Chem.* **2009**, *48*, 9419. (m) Fortier, S.; Wu, G.; Hayton, T. W. *Inorg. Chem.* **2009**, *48*, 3000. (n) Lam, O. P.; Anthon, C.; Meyer, K. *Dalton Trans.* **2009**, 9677. (o) Broderick, E. M.; Gutzwiller, N. P.; Diaconescu, P. L. *Organometallics* **2010**, *29*, 3242. (p) Fortier, S.; Wu, G.; Hayton, T. W. *Dalton Trans.* **2010**, *39*, 352.

(11) (a) Wang, J. X.; Dash, A. K.; Kapon, M.; Berthet, J. C.; Ephritikhine, M.; Eisen, M. S. *Chem. Eur. J.* **2002**, *8*, 5384. (b) Hayes, C. E.; Leznoff, D. B. *Organometallics* **2010**, *29*, 767. (c) Hayes, C. E.; Platel, R. H.; Schafer, L. L.; Leznoff, D. B. *Organometallics* **2012**, *31*, 6732.

(12) (a) Jantunen, K. C.; Batchelor, R. J.; Leznoff, D. B. *Organometallics* **2004**, *23*, 2186. (b) Cruz, C. A.; Emslie, D. J. H.; Harrington, L. E.; Britten, J. F.; Robertson, C. M. *Organometallics* **2007**, *26*, 692.

(13) Jantunen, K. C.; Haftbaradaran, F.; Katz, M. J.; Batchelor, R. J.; Schatte, G.; Leznoff, D. B. *Dalton Trans.* **2005**, 3083.

(14) Wilson, D. J.; Sebastian, A.; Cloke, F. G. N.; Avent, A. G.; Hitchcock, P. B. *Inorg. Chim. Acta* **2003**, *345*, 89.

(15) Note also that the 0.58 factor customarily used to correct the M_n values of PLLA samples determined against poly(styrene) standards, as done in this study, are generally grossly underestimated for high-

molecular-weight polymer (such as those given in Table 1, entries 4 and 12); a higher factor is more likely to be correct and would result in higher values of M_n(SEC).
(16) The trimethylsilyl group α to a ketone is known to undergo facile elimination under a variety of reaction conditions. See for instance: (a) Demuth, M. *Helv. Chim. Acta* **1978**, *61*, 3136. (b) Chan, T.-H.; Chang, E.; Vinokur, E. *Tetrahedron Lett.* **1970**, *14*, 1137. (c) Fleming, I.; Dunogues, J.; Smithers, R. *Org. React.* **1989**, 37.
(17) (a) Miao, W.; Li, S.; Zhang, H.; Cui, D.; Wang, Y.; Huang, B. *J. Organomet. Chem.* **2007**, *692*, 4828. (b) Yang, Y.; Cui, D.; Chen, X. *Dalton Trans.* **2010**, *39*, 3959. (c) Otero, A.; Fernandez-Baeza, J.; Sanchez-Barba, L. F.; Tejeda, J.; Honrado, M.; Garces, A.; Lara-Sanchez, A.; Rodriguez, A. M. *Organometallics* **2012**, *31*, 4191.
(18) Hermann, J. A.; Suttle, J. F. *Inorg. Synth.* **1957**, *5*, 143.
(19) Arunachalampillai, A.; Crewdson, P.; Korobkov, I.; Gambarotta, S. *Organometallics* **2006**, *25*, 3857.
(20) (a) Elias, A. J.; Roesky, H. W.; Robinson, W. T.; Sheldrick, G. M. *J. Chem. Soc., Dalton Trans.* **1993**, 495. (b) Male, N. A. H.; Thornton-Pett, M.; Bochmann, M. *J. Chem. Soc., Dalton Trans.* **1997**, 2487.
(21) Aizenberg, M.; Turculet, L.; Davis, W. M.; Schattenmann, F.; Schrock, R. R. *Organometallics* **1998**, *17*, 4795.
(22) Betteridge, P. W.; Carruthers, J. R.; Cooper, R. I.; Prout, K.; Watkin, D. J. *J. Appl. Crystallogr.* **2003**, *36*, 1487.
(23) Farrugia, L. J. *J. Appl. Crystallogr.* **1997**, *30*, 565.
(24) *Persistence of Vision Raytracer, version 3.6.1*; Persistence of Vision Pty. Ltd., Williamstown, Victoria, Australia, 2004.